Penerbit Akademia Baru

Journal of Advanced Research in Experimental Fluid Mechanics and Heat Transfer

Journal homepage:
http://www.akademiabaru.com/submit/index.php/arefmht
ISSN: 2756-8202

Eliminating Drag and Optimizing Motion by Configuration Foils on Pentamaran

Purwo Joko Suranto[1], Wiwin Sulistyawati[1,*], Fajri Ashfi Rayhan[1], Muhammad Iqbal[1], Ardi Nugroho Yulianto[2]

[1] Naval Engineering, Faculty of Engineering, University of Pembangunan Nasional Veteran Jakarta, Depok 16515, Indonesia
[2] Naval Architecture Department, Institut Teknologi Sepuluh Nopember, Surabaya 60111, Indonesia

ARTICLE INFO

Article history:
Received 20 March 2025
Received in revised form 12 April 2025
Accepted 10 May 2025
Available online 30 June 2025

Keywords:
Dual foils; NACA 0012; pentamaran; drag reduction; motion

ABSTRACT

Hydrodynamic efficiency is important in ship design to reduce the drag and improve performance. Altering the shape of a ship and enhancing its structure are some of the most common methods to improve hydrodynamic performance. The objective of this study is to assess the impact of having dual NACA 0012 foils on a pentamaran's hydrodynamic performance in terms of drag reduction and motion control. Dual foils are configured with varying vertical spacing but are kept at a similar horizontal position. The analysis evaluated the computational and experimental investigation of total drag under foil and no-foil. The foils reduce drag by 33% over the non-foiled configuration while increasing the lift by 4.4%. Moreover, compared to the monohull, the pentamaran with double foils exhibited better motion stability, decreasing the heave by 1.1%–2.5% and pitching by 0.18%–0.3%. Overall, the research indicates that those dual foils substantially improve the pentamaran hydrodynamics—throwing some light on the potential for optimizing the multihull for fuel consumption.

1. Introduction

Ship research has made many improvements to increase efficiency with decreasing drag. Optimization in hull form minimizes wave drag using streamlined shapes and bulbous bows [1-4]. The air lubrication systems research by Ceccio [5], Jang *et al.,* [6], Kim *et al.,* [7] and Putranto *et al.,* [8], including methods such as microbubble injection and air cavity systems, decrease skin friction by introducing a low-friction air layer under the hull. Hydrofoil research could be found by Bøckmann *et al.,* [9], D'Amato *et al.,* [10], Moreira *et al.,* [11] and Ghadimi *et al.,* [12], which administratively lifts parts of the hull out of the water, reducing wetted surface area and drag.

Foils on multihulls, particularly hydrofoils, have transformed the efficiency and performance of these ships by significantly reducing drag and maximizing movement. As foils generate lift, this reduces the wetted surface area, creating less frictional drag and allowing for greater speed and

* *Corresponding author.*
E-mail address: wiwinsulistyawati@upnvj.ac.id (Wiwin Sulistyawati)

https://doi.org/10.37934/arefmht.20.1.91101

efficiency. The use of hydrofoils on multihulls has many benefits. Well-researched studies have proven that hydrofoils reduce fuel consumption, increase operational efficiency and safer overall on-the-water practices. The flapping foil was applied to a ship propulsion scenario where an active flapping foil, simplifying from natural biology, showed 5% better performance than a screw propeller because of a larger working area [13]. Research by Belibassakis *et al.,* [14] and Priovolos *et al.,* [15] investigated the effect of foil configuration on thrust generation. Their results showed significantly increased propulsion efficiency was possible under usual operating conditions. Then anderson *et al.,* [16] studied and tested the NACA 0012 foil profile to analyse the hydrofoil flow and wake. They concluded that their high propulsive efficiency was 87% based on their findings. Then, Faltinsen [17] details the basic hydrodynamic mechanics of hydrofoils. They were processed and framed within numbers from Guglielmini *et al.,* [18], derived from the same ideas by Wang [19] and showing evidence, that even greater thrust values can be obtained by adding pitching oscillations to the heaving of the foil. While Moreira *et al.,* [20] explored the potential of a dual-flapping foil system for propulsion and energy harvesting. Nevertheless, previous studies have not adequately investigated how dual-flapping foils can be utilized in pentamaran hulls. Although such foils have been studied for their propulsion and energy-harvesting potential, their unique effects on pentamaran hydrodynamics are unknown.

The research concludes that dual flapping foils in unaligned configurations can effectively be used for propulsion and wave energy conversion. Based on the dual flapping foil system researched by Moreira *et al.,* [11], this research presents a promising advancement for the pentamaran. The foils, with a width corresponding to the main hull of the pentamaran, are positioned at a distance of Lx from the midship of the hull. In this study, variations were carried out on the distance of the dual foils with NACA 0012, with variation x-axis (Lx) and y-axis on the height of the dual foils (Ly). The pentamaran model of the current study is based on the works of Sulistyawati *et al.,* [21-23], which are further developments of the corresponding author's research in this area from 2018.

2. Theoretical

2.1 Dual Foils System

In the present research, two foils with 0^o angle of attack placed in an unaligned configuration, separated by horizontal and vertical distances of Lx and Ly, are presented in Figure 1 with position variations, as shown in Table 1. Eq. (1) and Eq. (2) give the relations used to determine the hydrodynamic coefficients for lift (C_L) and drag (C_T):

$$C_T = \frac{T}{\frac{1}{2}\rho V_\infty^2 bc} \tag{1}$$

$$C_L = \frac{L}{\frac{1}{2}\rho V_\infty^2 bc} \tag{2}$$

where ρ is the fluid density, V is a ship's relative velocity, b is the foil span and c is the foil chord. Eq. (3) shows that the hydrofoil functions as a wave energy converter to the power:

$$P = {}^1\!/_2\, \rho V_\infty^3 bd \tag{3}$$

where d, which relates to the amplitude of both the wave and the foil, represents the total vertical motion. Regarding energy transfer, JONSWAP with regular wave heights is represented by sinusoidal

functions, which significantly simplifies the model by using a regular wave model. A generic regular wave function is represented as:

$$H(t) = Asin(\omega t + \emptyset) \tag{4}$$

where *H* denotes the elevation, *ω = 2pf*, the angular frequency, *A* represents the wave amplitude and ϕ is the phase. At the foil sites in a future ship-attached system, the foil motion is directly connected to the wave elevation, comparable to the Response Amplitude Operator (RAO). The functions that represent the angular location and velocity for each foil in the pitching action are as follows:

$$\Omega_1(t) = \theta_0 \gamma \cos(\omega_e t) \tag{5}$$

$$\Omega_2(t) = \theta_0 \gamma \cos(\omega_e t + \phi_{12}) \tag{6}$$

The pitch amplitude is represented by θ_0, the individual foil angular velocities are Ω1 and Ω2 and the frequency is denoted by ωe= ω+ kV∞, where k is the wave number and the phase between foils is denoted by ϕ12.

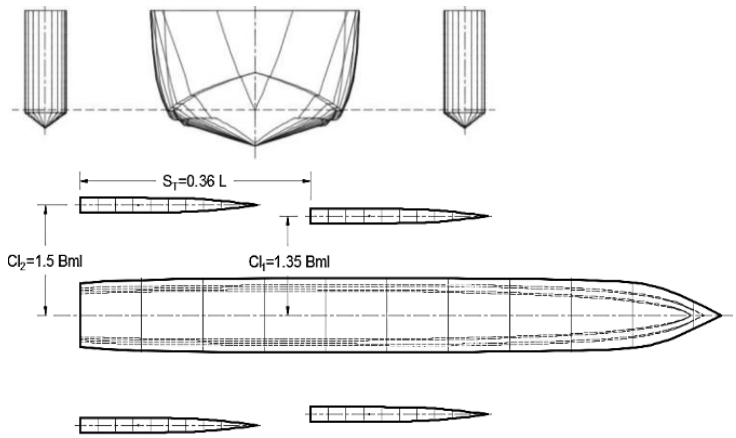

(a) Model pentamaran

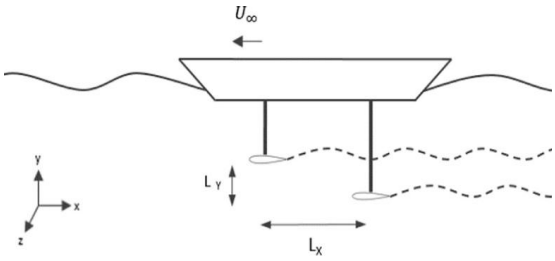

Model	*Lx*	*Ly*
Penta1	2 cords	1 cord
Penta2	2 cords	0,7 cord
Penta3	2 cords	0,5 cord

(b) Variation position NACA 0012

Fig. 1. Model pentamaran and setup NACA 0012 configuration based on research of Moreira *et al.,* [11]

Table 1
Principle dimensions of Pentamaran

Dimension	Main hull	Side hull
Length (L)	1435.9 mm	414 mm
Beam (Bml)	126.7 mm	30 mm
Draft (T)	24 mm	12 mm
Height (H)	90 mm	78 mm
Deadrise (degree)	20	35
Wetted area (mm^2)	17.68×10^4	14.87×10^3
Displacement (mm^3)	20.45×10^5	69.01×10^3

2.2 CFD Simulation

By ITTC requirements 2011, this investigation employed commercial ANSYS 2021 CFD software. The boundary for drag analysis was one length of perpendicular (Lpp) from the bow, which marked the domain boundary of the inlet and two Lpp from the stern, which marked the outflow. The top was placed 0.5 Lpp from the keel, the bottom 1 Lpp from the keel and the side at 1 Lpp from the

plane of symmetry. According to the foil literature, a symmetrical shape is preferred and it should be kept as thin as possible to prevent needless residual drag forces [24,25].

The analytical result of drag was verified using the converged number of meshing elements and a numerical uncertainty assessment. A combination of prismatic and tetrahedral cells has been meshing with unstructured features. The element sizes were changed from 0.1 to 0.035 to 0.01 for both the ship hull and the boundary. Throughout the meshing process, the value of Y^+ was considered regarding the total number of components and mesh size; that basic mesh produced 5.02 million components, which grew to 16.3 million. The wall function for turbulence models was set using a hybrid technique, in which y+ > 30 was used for the wall functions and y+≈ 1 was used for the initial near-wall grid point of the ship boundary conditions. The simulations included the shear-stress transport (SST) model, a widely used turbulence model in hydrodynamic evaluations of ships. As stated by Ferziger *et al.,* [26], the SST model consists of a k-ω formulation for the inner boundary layer and a modified k-ω model for the free stream and outer boundary layer.

The parameters assessed in motion analysis using AQWA on RAO (Response Amplitude Operator) to determine the prediction of motion characteristics of heaving and pitching movements in the direction of head seas waves (180 degrees). Chakrabarti [27] state that RAO is a transfer function that allows a structure to respond to external loads (waves). The following is the RAO equation in the frequency function:

$$RAO = \left(\frac{Ra}{\zeta a}\right)^2 \tag{7}$$

where $[RAO(\omega e)]^2$ is the response Amplitude Operator (RAO), Ra is the amplitude of motion response [m] and ζa is the amplitude of wave [m].

3. Results

3.1 Drag Investigation

Figure 2 and Figure 3 compare Pentamaran dual foils and those without foil by simulation and tests. Including foils in the pentamaran significantly improves hydrodynamic performance, reducing drags. Foils are particularly effective at higher Froude numbers, where drag coefficients for configurations with foils are much lower than those without foils.

In Figure 2(a), the largest discrepancy of simulation to experimental values was at Fn=0.35 (24.62%) and the smallest discrepancy was at Fn=0.70 (17.78%). For each configuration, total drag is shown to drop as Fn is increased, suggesting a reduction in drag relative to velocity. The differences between Penta1, Penta2 and Penta3 demonstrate how hull shape and foil arrangement affect drag. A comparison of CFD and experimental results for pentamaran without dual foils is presented in Figure 2(b), clearly indicating the significant deviations, especially evident in wave drag (C_W), as the CFD approach tends to underestimate wave-induced effects.

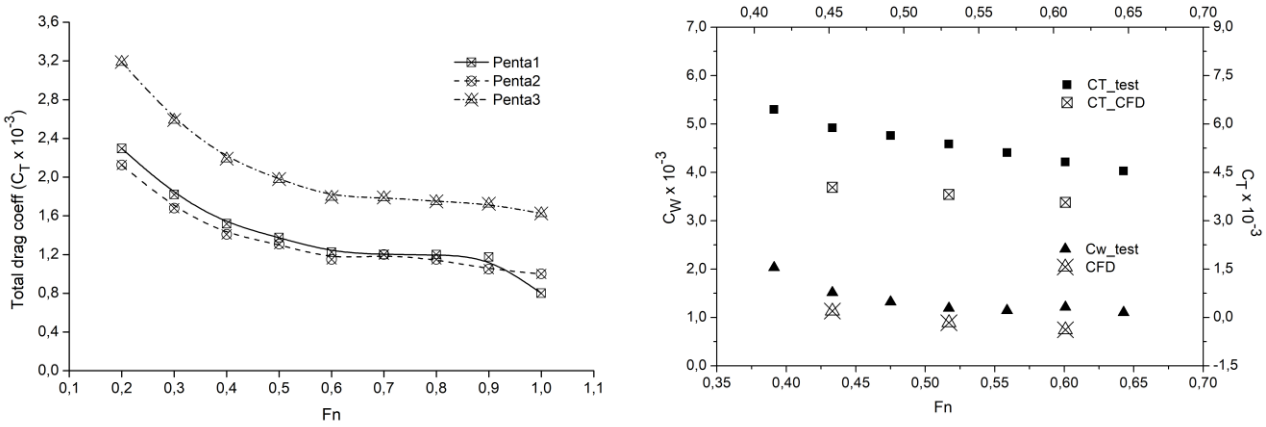

(a) Coefficient total drag of pentamaran by CFD simulation

(b) Coefficient total drag of pentamaran without dual foils by CFD simulation and test

Fig. 2. Comparison of total drag coefficient of Pentamaran dual foils and without foil

Figure 3(a) shows that the friction coefficient (CF) decreases with increased Fn due to thinner boundary layers. Penta3 had the highest friction, followed by Penta1 and Penta2, with lower numbers indicating the hull geometry played a role in skin friction. Figure 3(b) shows results comparing simulation and experimental data for a pentamaran without dual foils, where data points diverge due to limitations with CFD that cannot accurately model viscous effects that are prominent at low speeds.

Figure 2 and Figure 3 have a close relationship, emphasizing the basic connection between total drag and the components that contribute to it — wave and frictional drag. Since skin friction accounts for a large portion of hydrodynamic drag, the friction coefficient directly impacts the total drag behaviour. The discrepancies between the CFD and experimental values in both figures highlight the need for further modelling, particularly to account for wave effects and viscous interactions.

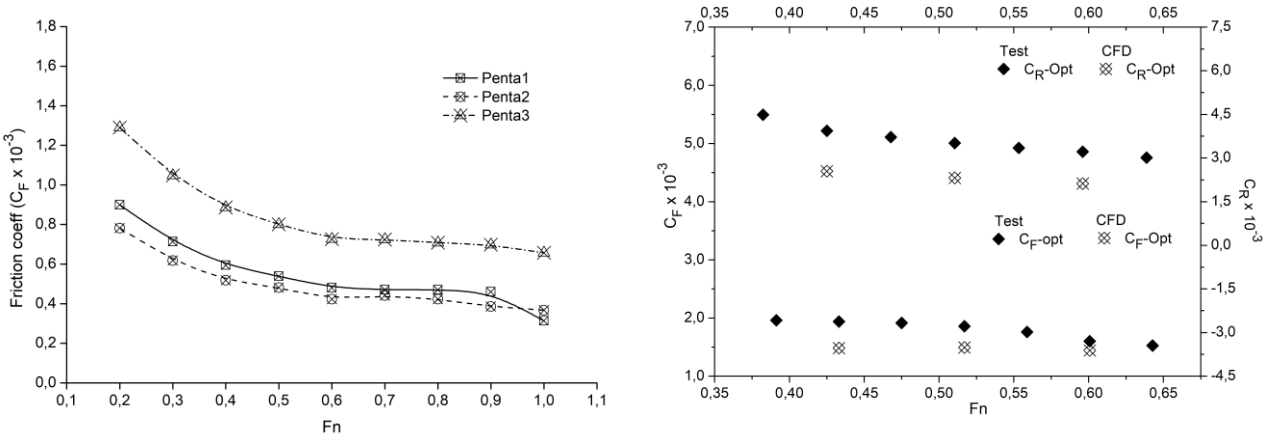

(a) Friction coefficient of pentamaran by CFD simulation

(b) Coefficient friction of pentamaran without dual foils by CFD simulation and test

Fig. 3. Comparison of friction coefficient of pentamaran dual foils and without foil

Peak lift potential & wave drag analysis for Pentamaran (Figure 4) shows the wave drag and lift performance of the three pentamarans. The Froude number (Fn) negatively affects the wave coefficient (C_w). Penta1 has the best wave drag characteristics of all the designs, with the lowest wave coefficient at all speeds. Wave drag is the highest for Penta3 and the most inefficient configuration. The lift coefficient (C_T/C_L) is increased with the Fn increase, where the higher lift is produced in the case of Penta3, which Penta2 closely follows, while the lift coefficient for Penta1 is

the lowest. Overall, these results indicate that Penta1 is the highest performer in reducing wave drag, thus making it a good candidate for more fuel-efficient and stable applications. On the flip side, the Penta3 configuration allows for the highest lift coefficient, which can be useful for dynamic lift applications but introduces significant wave drag.

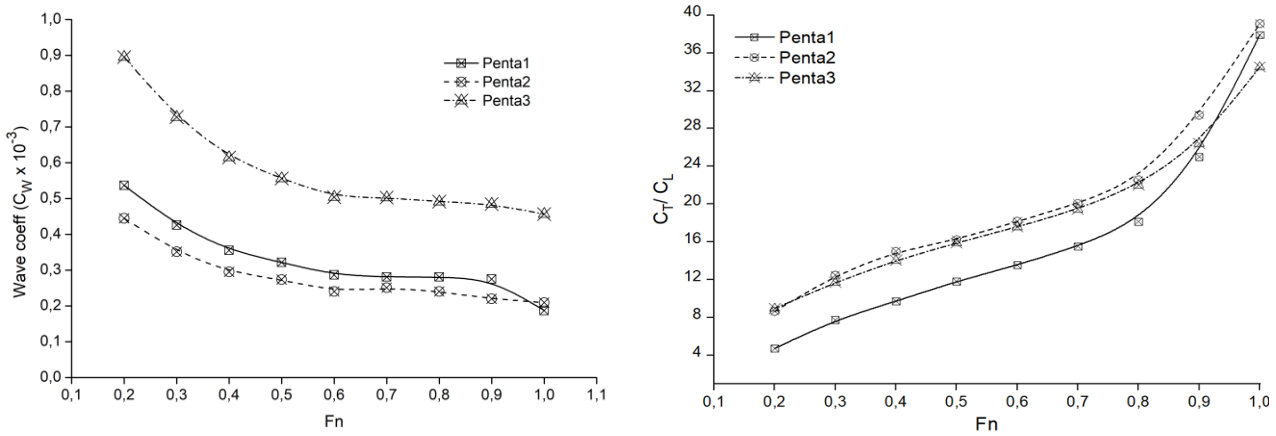

(a) Wave coefficient of pentamaran by CFD simulation (b) Lift coefficient of pentamaran by CFD simulation

Fig. 4. Comparison of wave and lift coefficient of pentamaran dual foils by CFD simulation

For pentamaran hull forms, the interaction of the wakes and the resulting formation of vortices play a leading role in drag mitigation and enhanced lift. The wake of the interference is greatly affected by the number and spacing of the hulls, with an optimized arrangement resulting in reduced energy being wasted in turbulent mixing. This configuration minimizes damaging wake interactions and stabilizes flow separation, which Penta1 indicates with the lowest drag. In contrast, Penta3 suffers from more drag , indicating stronger vortex shedding and unsteady wake attributes that increase the drag. At lower Froude numbers, strong vortex-induced drag indicates poor energy dissipation. Conversely, the lift-to-drag ratio improves with increasing Froude numbers, suggesting that vortex structures behind the foil have more stability and enhanced lift generation. Controlled vortex formations on Penta1 promote pressure recovery, improving lift and efficiency.

3.2 Heave Motion

AQWA has been used for heave and pitch motion analysis, as illustrated in Figure 5 and Figure 6. Following sea (0°), stern quartering sea (45°), beam sea (90°) and head sea (180°) are examined for both motions in wave direction. In Figure 5(a), where they do have some degree of difference, they seem minor; Penta1 appears to have slightly higher heave amplitudes than Penta2 or Penta3. The trends are closely similar to the following sea, Figure 5(b), with a large amplitude response at the low-frequency end of the spectrum and a secondary peak centred around ~1.0 - 1.2 Hz. That indicates the pentamaran reacts similarly in following and head sea and the different configurations' heave motion is relatively close.

For beam sea, Figure 5(c), significant differences can be observed in this condition compared to Figure 5(a) and 5(b). The maximum amplitude increases (~1.6 m/m) at approximately 1.0 Hz, suggesting increased resonance in beam seas. Similar trends are observed in all three configurations, but Penta3 shows lower heave amplitudes, indicating increased stability of beam waves. Initially, in the stern quartering sea, Figure 5(d), heave motion decreases continuously with frequency in the previous cases. There is lower decay in the response and differences between Penta1, Penta2 and

Penta3. That means the pentamaran hull has lower sensitivity to stern quartering waves, so the resonance effects are lower.

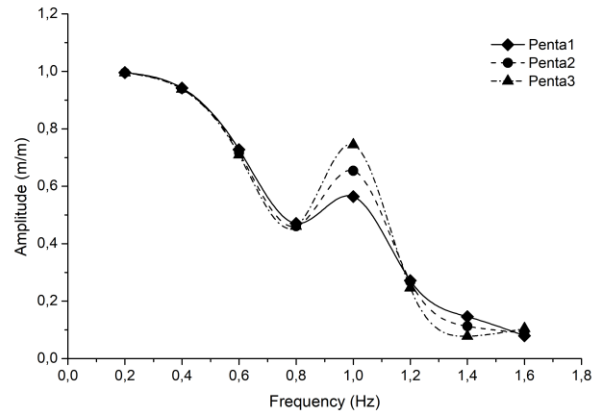

(a) Heave motion (m/m) on the following sea at wave direction 0°

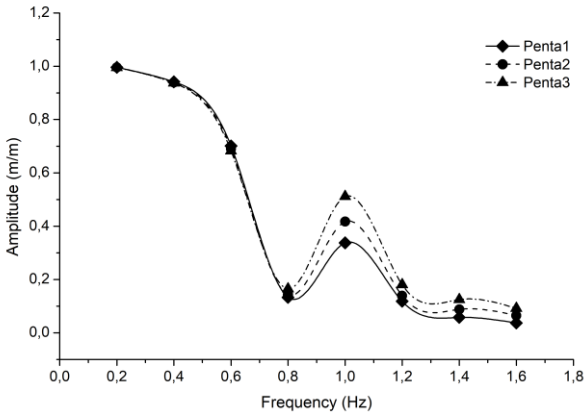

(b) Heave motion (m/m) on the head sea at wave direction 180°

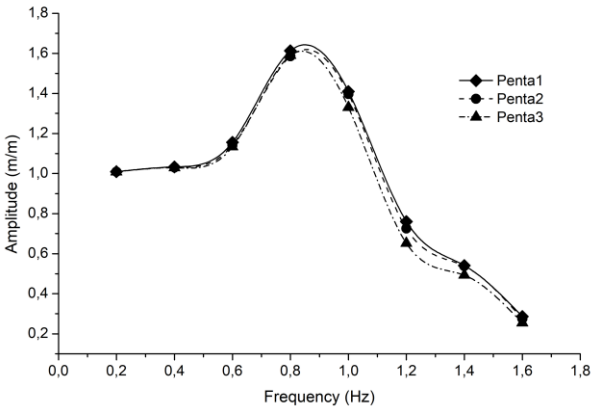

(c) Heave motion (m/m) on the beam sea at wave direction 90°

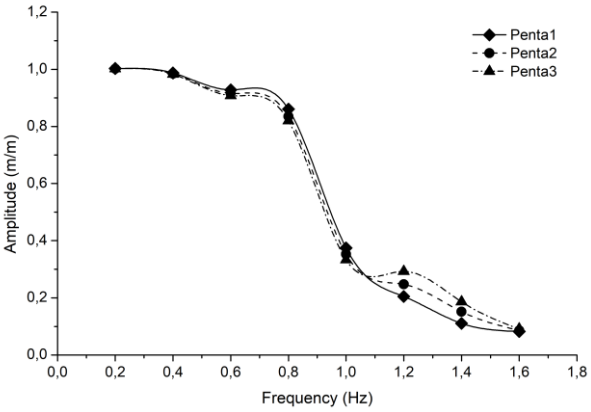

(d) Heave motion (m/m) on the stern quartering sea at wave direction 45°

Fig. 5. Heave motion pentamaran (m/m) at wave direction 0, 90°, 45 ° and 180 °

3.3 Pitch Motion

Observed on pitch motion, Figure 6(a), the amplitude peak of Penta1 is 0.7 Hz, much larger than others. Penta2 and Penta3 show similar trends, but their peaks' amplitudes are below that of Penta1. All configurations exhibit a rapid decrease in pitch motion at a frequency greater than 1.0 Hz. As the head sea, Figure 6(b) follows a similar trend concerning peak amplitude, with Penta 1 showing the largest peak amplitude. The differences between the peak amplitudes of the configurations are not as evident. At higher frequencies (> 1.0 Hz), the pitch amplitudes for all configurations tend to converge. At beam sea, Figure 6(c), all configurations present a wider amplitude response with a gentler rise and decline than before. The differences between Penta1, Penta2 and Penta3 are smaller, signalling that the behaviour is more consistent between the configurations under beam sea conditions. In Figure 6(d), quartering sea, Penta1 again shows the highest peak amplitude. The peak appears at the same frequency (0.7-0.8 Hz) as the other headings. After the peak, the amplitudes of all configurations decrease quickly and converge.

Penta 1 has a 1.6% higher pitch than Penta 2 and a 7.4% higher pitch than Penta 3, showing that Penta 3 generates the least pitch and more stability in beam seas can be found. Penta 1 is, on average,

pitched 0.7% forward of Penta 2 (0.6% versus Penta 3 in stern quartering sea), indicating that differences in pitch tend to be small in stern quartering waves. However, the Penta 3 is the most stable configuration. Due to its relatively low block coefficient, Penta 3 has the highest pitch stabilizing effect in all wave directions. As shown, P1 has the highest pitch, particularly in the head, beam, and stern quartering seas and tends to pitch, thus making it less stable. Differences in pitch are more apparent in head and beam seas than in following and stern quartering.

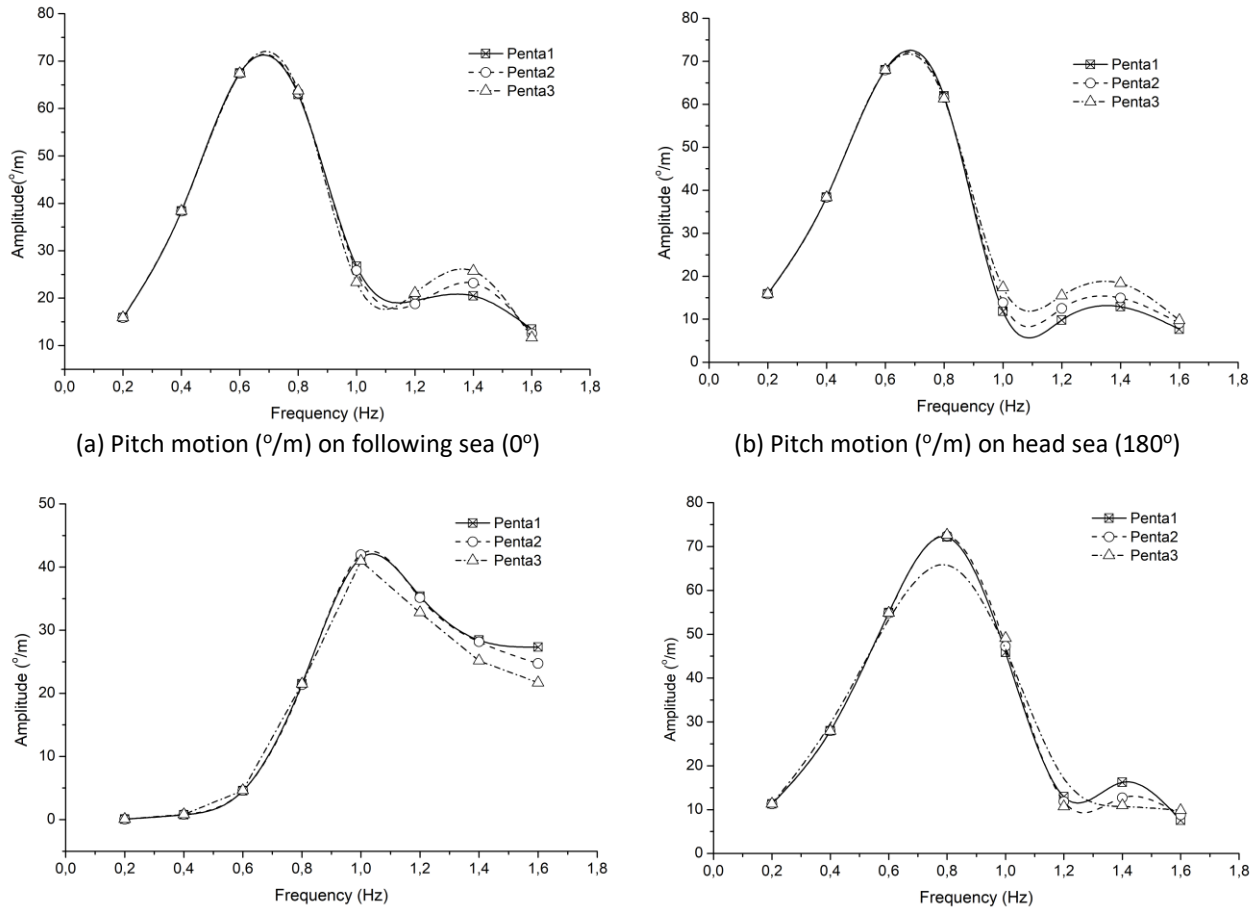

(a) Pitch motion (°/m) on following sea (0°)

(b) Pitch motion (°/m) on head sea (180°)

(c) Pitch motion (°/m) on beam sea (90°)

(d) Pitch motion (°/m) on stern quartering sea (45°)

Fig. 6. Pitch motion pentamaran (rad/m) at wave direction 0, 90°, 45 ° and 180 °

3.4 Wave Contour

The wave contour of the CFD simulation at Fr 0.1 is plotted on a pentamaran with dual foils (a,b,c) and capturing contour from the experiment without dual foil (Figure 8). 'More Giant Waves' with dark blue colours than other light blue colours and evidence a pentamaran with double foil at Ly 1 cord produce a great wave then Ly.0.5 cord and 0.7 cord. The total drags outcomes shown in Figure 2 for the Ly 1 cord (penta3) were superior to the two models. Contour differences of waves from CFD simulation results show that the pentamaran installed with different positions dual foils (Ly 0.5, 0.7 and 1 chord) has a variety of wave shapes, in which the Ly 1 chord wave effect is the most prominent. As seen above, the wave generation pattern is consistent with the total drag results shown in Figure 2; the Ly 1 chord (Penta3) configuration has the largest drag out of the discussed models. A higher chord would create a greater wave effect and increase the overall drag than the Ly 0.5 and 0.7 chord positions.

The experiment on the pentamaran was conducted at the Institut Teknologi Sepuluh Nopember (ITS) towing tank in Indonesia, which is 50 m long, 3 m wide and 2 m deep. But dual-foiled pentamarans have not yet been tested. An effective transverse wave dampening can be observed behind the front hull centreline in the experimental setup without foils (Figure 8) for a hull configuration with main and front hull centrelines angled 18° against each other. This setup helps to minimize wave and total drag. The wave height reduction is consistent with previous research involving arrow tri-hull ships, suggesting that optimal hull positioning can improve hydrodynamic performance. These results indicate that optimum hull angles can drastically improve drag behaviour. Future experimental studies on pentamaran with dual foils are needed to quantify the agreement with the CFD and whether similar benefits would arise with the addition of foils. The experimental on-interference perspective gives insight into wave interactions between hulls that could correlate with the simulations to study each simulation's drag and stability.

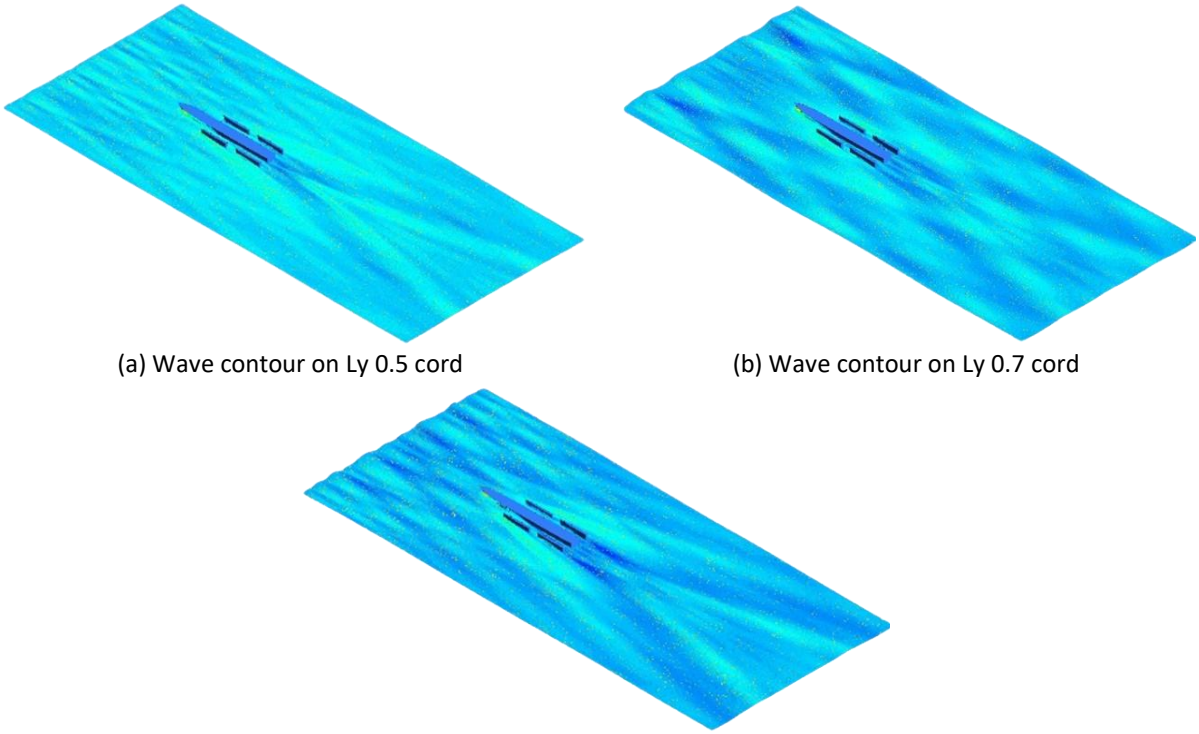

(a) Wave contour on Ly 0.5 cord (b) Wave contour on Ly 0.7 cord

(c) Wave contour on Ly 1 cord

Fig. 7. Wave contour simulation at Fn 1.0 on Pentamaran with dual foil: (a) Wave contour on Ly 0.5 cord (b) Wave contour on Ly 0.7 cord (c) Wave contour on Ly 1 cord

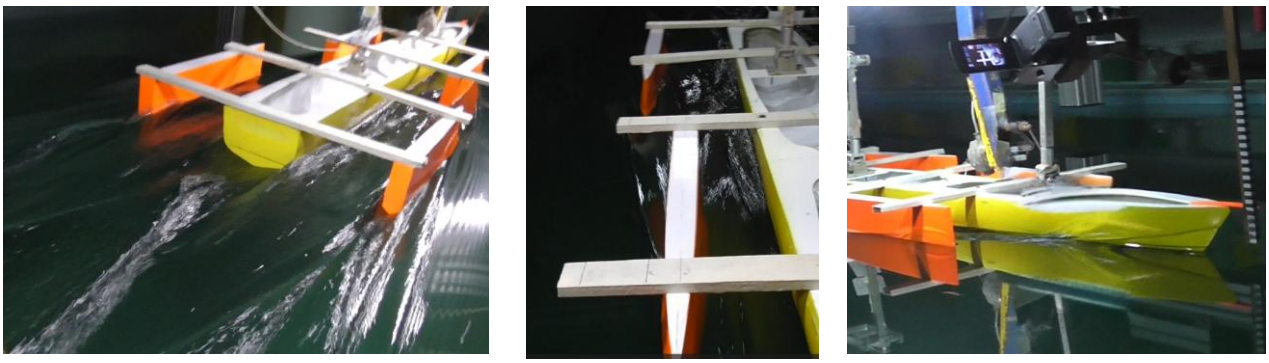

(a) Stern view (b) Interference view (c) Front view

Fig. 8. Capturing the wave contour of pentamaran from the test

4. Conclusion

This unique concept introduces a novel approach to hull design, leveraging dual foils in a pentamaran configuration to minimize drag and seakeeping. In this study, the effects of NACA 0012 dual foils on a pentamaran were analysed with varying NACA foil vertical distances (Ly) while keeping the horizontal placement (Lx) constant. The results were computationally and experimentally compared to both foil and non-foil cases. As this study demonstrates, how foil is placed is crucial to optimizing hydrodynamic efficiency; placing a foil of Ly 0.5 and Lx 0.7 chords was the most effective configuration. As with all multihulls, positioning the hulls relative to each other aids in performance enhancements. Based on the simulation's result, the study determined that a 2-chord horizontal spacing (Lx) and 0.5-chord vertical distance (Ly) configuration provides a 33% total drag reduction compared to a pentamaran without foils. Indicating that dual foils effectively reduce drag. The foils produced lift force, which increased the lift by 4.4%. The Pentamaran dual foils scheme yielded the best reduction in motion with heave 1.1% - 2.5% and pitch reduced 0.18% - 0.3%. This study also has shown the effect of hull design on pitch motion response, with Penta1 being generally more susceptible to higher pitch motion, particularly in the condition of following and head seas. A comparison between CFD simulation and the experimental test data showed maximum deviation at lower speeds (Fn = 0.35) and is slightly lower at higher speeds (Fn = 0.65). If efficiency and lower wave drag (e.g., fuel savings and better stability) are of utmost importance, then Penta1 is the way to go. With higher lift and dynamic performance requirements, Penta3 may be the preferred choice.

This report demonstrated the qualitative performance difference to some degree; future work would be needed to validate these results in complex tests. Sea trials, structural fatigue studies and feasibility evaluations are also important to facilitate the incorporation of such findings into marine technology.

Acknowledgement
The authors thank Universitas Pembangunan Nasional (UPN) Veteran Jakarta for providing financial support through the 2024 RISCOP Grant Programme. We would also like to thank our research colleagues and collaborators for their helpful input and technical assistance during the research.

References

[1] Cheng, Xide, Baiwei Feng, Zuyuan Liu and Haichao Chang. "Hull surface modification for ship resistance performance optimization based on Delaunay triangulation." *Ocean Engineering* 153 (2018): 333-344. https://doi.org/10.1016/j.oceaneng.2018.01.109

[2] Miao, A. Q. and D. C. Wan. "Multi-objective optimization of ship wave-making resistance based on MOPSO." *Chinese Journal of Hydrodynamic* 34, no. 3 (2019): 291-298.

[3] Zhang, Shenglong, Tahsin Tezdogan, Baoji Zhang and Ling Lin. "Research on the hull form optimization using the surrogate models." *Engineering Applications of Computational Fluid Mechanics* 15, no. 1 (2021): 747-761. https://doi.org/10.1080/19942060.2021.1915875

[4] Shichao, W. A. N. G. and L. I. U. Gang. "Efficient ship hull multi-objective optimization method considering ice resistance and calm water resistance." *Chinese Journal of Ship Research* 19, no. 6 (2024): 97-107.

[5] Ceccio, Steven L. "Friction drag reduction of external flows with bubble and gas injection." *Annual Review of Fluid Mechanics* 42, no. 1 (2010): 183-203. https://doi.org/10.1146/annurev-fluid-121108-145504

[6] Jang, Jinho, Soon Ho Choi, Sung-Mok Ahn, Booki Kim and Jong Soo Seo. "Experimental investigation of frictional resistance reduction with air layer on the hull bottom of a ship." *International Journal of Naval Architecture and Ocean Engineering* 6, no. 2 (2014): 363-379. https://doi.org/10.2478/IJNAOE-2013-0185

[7] Kim, Young-Rong and Sverre Steen. "Potential energy savings of air lubrication technology on merchant ships." *International Journal of Naval Architecture and Ocean Engineering* 15 (2023): 100530. https://doi.org/10.1016/j.ijnaoe.2023.100530

[8] Putranto, Vicky Adrian, Utomo, Allessandro and Gunawan. "Interaction Analysis of Micro Bubbles in the Flat Plate to Reduce drag using Computational Fluid Dynamic." Semarak Engineering Journal, 4 no 1 (2024): 18–28.
[9] Bøckmann, Eirik and Sverre Steen. "Model test and simulation of a ship with wavefoils." *Applied Ocean Research* 57 (2016): 8-18. https://doi.org/10.1016/j.apor.2016.02.002
[10] D'Amato, Egidio, Immacolata Notaro, Vincenzo Piscopo and Antonio Scamardella. "Hydrodynamic design of fixed hydrofoils for planing craft." *Journal of Marine Science and Engineering* 11, no. 2 (2023): 246. https://doi.org/10.3390/jmse11020246
[11] Moreira, Diego, Nuno Mathias and Tiago Morais. "Dual flapping foil system for propulsion and harnessing wave energy: A 2D parametric study for unaligned foil configurations." *Ocean Engineering* 215 (2020): 107875. https://doi.org/10.1016/j.oceaneng.2020.107875
[12] Ghadimi, Aliakbar, Hassan Ghassemi and Parviz Ghadimi. "Hydrodynamic improvement of trimarans through multiple foils for trim control, resistance reduction and wake attenuation in planing operations." *Physics of Fluids* 37, no. 2 (2025). https://doi.org/10.1063/5.0254524
[13] Yamaguchi, H. and N. Bose. "Oscillating foils for marine propulsion." In *ISOPE International Ocean and Polar Engineering Conference*, pp. ISOPE-I. ISOPE, 1994.
[14] Belibassakis, K. A. and E. S. Filippas. "Ship propulsion in waves by actively controlled flapping foils." *Applied Ocean Research* 52 (2015): 1-11. https://doi.org/10.1016/j.apor.2015.04.009
[15] Priovolos, A. K., E. S. Filippas and K. A. Belibassakis. "A vortex-based method for improved flexible flapping-foil thruster performance." *Engineering Analysis with Boundary Elements* 95 (2018): 69-84. https://doi.org/10.1016/j.enganabound.2018.06.016
[16] Anderson, Jamie M., K. Streitlien, D. S. Barrett and Michael S. Triantafyllou. "Oscillating foils of high propulsive efficiency." *Journal of Fluid mechanics* 360 (1998): 41-72. https://doi.org/10.1017/S0022112097008392
[17] Faltinsen, Odd M. *Hydrodynamics of high-speed marine vehicles*. Cambridge university press, 2005. https://doi.org/10.1017/CBO9780511546068
[18] Guglielmini, Laura and Paolo Blondeaux. "Propulsive efficiency of oscillating foils." *European Journal of Mechanics-B/Fluids* 23, no. 2 (2004): 255-278. https://doi.org/10.1016/j.euromechflu.2003.10.002
[19] Wang, Z. Jane. "Vortex shedding and frequency selection in flapping flight." *Journal of Fluid Mechanics* 410 (2000): 323-341. https://doi.org/10.1017/S0022112099008071
[20] Moreira, Diego, Nuno Mathias and Tiago Morais. "Dual flapping foil system for propulsion and harnessing wave energy: A 2D parametric study for unaligned foil configurations." *Ocean Engineering* 215 (2020): 107875. https://doi.org/10.1016/j.oceaneng.2020.107875
[21] Sulistyawati, Wiwin, Yanuar Yanuar and Agus Sunjarianto Pamitran. "Research on pentamaran by model test and theoretical approach based on Michell's integral." *CFD Letters* 11, no. 3 (2019): 117-128.
[22] Sulistyawati, Wiwin and P. Suranto. "Achieving Drag Reduction with Hullform Improvement in Different Optimizing Methods." *International Journal of Technology* 11, no. 7 (2020): 1370-1379. https://doi.org/10.14716/ijtech.v11i7.4468
[23] Sulistyawati, W. "CFD investigation of pentamaran ship model with chine hull form on the resistance characteristics." In *IOP Conference Series: Materials Science and Engineering*, vol. 316, no. 1, p. 012059. IOP Publishing, 2018. https://doi.org/10.1088/1757-899X/316/1/012059
[24] Kinsey, Thomas and Guy Dumas. "Parametric study of an oscillating airfoil in a power-extraction regime." *AIAA journal* 46, no. 6 (2008): 1318-1330. https://doi.org/10.2514/1.26253
[25] Xiao, Qing and Qiang Zhu. "A review on flow energy harvesters based on flapping foils." *Journal of fluids and structures* 46 (2014): 174-191. https://doi.org/10.1016/j.jfluidstructs.2014.01.002
[26] Ferziger, Joel H., Milovan Perić and Robert L. Street. *Computational methods for fluid dynamics*. springer, 2019. https://doi.org/10.1007/978-3-319-99693-6
[27] Chakrabarti, Subrata. "State of offshore structure development and design challenges." *Handbook of Coastal and Ocean Engineering* (2010): 667-694. https://doi.org/10.1142/9789812819307_0024